DEVELOPMENT OF THE LCLS-II OPTICS DESIGN *

Y. Nosochkov†, P. Emma, T. Raubenheimer, M. Woodley, SLAC, Menlo Park, CA 94025, USA

Abstract

The LCLS-II is a high repetition rate, high average brightness free-electron laser (FEL) under construction at the SLAC National Accelerator Laboratory. The LCLS-II will include new major components: a high repetition-rate injector, a superconducting, CW (continuous wave), 4-GeV linac with a bunch compressor system, a 3-way beam spreader, with independent hard X-ray (HXR) and soft X-ray (SXR) FEL undulators. The design is based on the existing SLAC facilities, including the LCLS linac and beam transport lines. The new SXR line will utilize a variable-gap undulator sharing the same tunnel with the new HXR horizontal-gap vertically polarizing undulator that will replace the existing LCLS undulator. We describe the current state of the electron optics design and the latest developments.

INTRODUCTION

The LCLS-II [1] free-electron laser (FEL) will be an upgrade of the existing Linac Coherent Light Source (LCLS) [2] at the SLAC National Accelerator Laboratory. It is designed to deliver high average brightness beams with up to 1 MHz repetition rate. The LCLS-II will be installed in the existing SLAC tunnel and will re-use the LCLS and PEP-II [3] transport lines. Horizontal layout of the LCLS-II, along with the LCLS linac and future FACET-II [4], is shown in Fig. 1.

The LCLS-II will include a new high repetition-rate (MHz) injector and a continuous wave (CW) superconducting RF (SCRF) 4-GeV linac installed in the first kilometer of the SLAC linac tunnel. The electron bunches will be compressed using bunch compressor chicanes and then transported through the existing 2-km PEP-II electron bypass line to a new 3-way beam spreader at the end of the LCLS linac. The spreader will provide high rate bunch-by-bunch deflection either into the new SXR (soft X-ray) or existing (LCLS) HXR (hard X-ray) transport lines, or towards the new 250-kW dump in the beam switch yard (BSY). The SXR and HXR beams then will be delivered to the new SXR and HXR variable-gap undulators installed side-by-side in the LCLS undulator hall. The LCLS-II will also retain the capability of delivering the 3-15 GeV beam from the existing 1-km LCLS 120-Hz Cu-linac (CuRF) to the HXR undulator. As a future option, the CuRF beam may be also delivered to the SXR undulator using an additional line in the spreader. The LCLS-II initial electron optics design has been previously reported in Ref. [5]. An updated design and the latest developments are presented here.

* Work supported by the Department of Energy Contract DE-AC02-76SF00515.

† yuri@slac.stanford.edu

SCRF LINAC

Schematic of the proposed 4-GeV SCRF linac is shown in Fig. 2. It will be based on existing technology developed for TESLA [6], ILC [7] and XFEL [8]. The linac includes 35 1.3-GHz cryomodules (CM) in the four main linac sections (L0, L1, L2, L3), a laser heater chicane (LH), a harmonic linearizer RF section (HL), and two bunch compressor chicanes (BC1, BC2). There is one 12-m long CM in L0, two in L1, 12 in L2, and 20 in L3. One CM includes eight 9-cell cavities (each $\simeq 1$ m long) resonant at 1.3-GHz, while the 3.9-GHz HL consists of two special CMs, each comprising of eight shorter 9-cell cavities. The average accelerating gradient is under 16 MV/m, with $\simeq 6\%$ overhead. The L3 cavities run on crest ($\phi = 0$) since the resistive-wall wake-field of the downstream 2-km bypass line removes the remnant energy chirp on the bunch. At the end of the SCRF linac, a linac extension section is reserved for future energy upgrade. The beam is transported for $\simeq 250$ m at which point it is directed up into the existing 2-km PEP-II electron bypass line. There is an off-axis diagnostic line just after the laser heater (at 100 MeV) into which the beam will be continuously deflected at a low rate ($\sim$100 Hz) for continuous beam diagnostics. This line will include the option for transverse deflecting cavities (TCAV) for an ongoing analysis of the beam time-sliced emittance and longitudinal phase space.

Optics functions of the main linac and the downstream extension section are shown in Fig. 3. The 30° FODO lattice in L2 and L3 uses cold quadrupole magnets at the end of each CM. Several warm quadrupoles around the bunch compressors provide a proper match of beta functions at these locations. This relatively weak FODO optics helps to reduce chromatic effects and loosens alignment tolerances and dispersion errors. The downstream extension section is made of 38-m long 45° FODO cells.

In order to drive the FELs, the 100-pC electron bunch is compressed in length by a factor of 100 to provide 1 kA of peak current. This is achieved with two four-bend compressor chicanes, BC1 and BC2, and a linear energy chirp on the bunch induced by off-crest RF phasing. The BC1 chicane is placed close to the injector, but at high enough energy (250 MeV) so that space charge forces do not degrade the beam brightness. The 3.9-GHz HL section before the BC1 removes the 2nd order chirp curvature. The BC2 chicane is placed at 1.6 GeV such that the remaining linear energy chirp (after compression) is canceled by the longitudinal wake-field of the accelerating cavities and the resistive-wall wake-field of the long bypass line. The R_{56} values of BC1 and BC2 are set to -55 mm and -37 mm, respectively, for optimal compression and minimal impact on the transverse emittance. Effects of coherent synchrotron radiation generated in the chicane bends are minimized by forcing a small horizontal beta function at the last chicane bend.

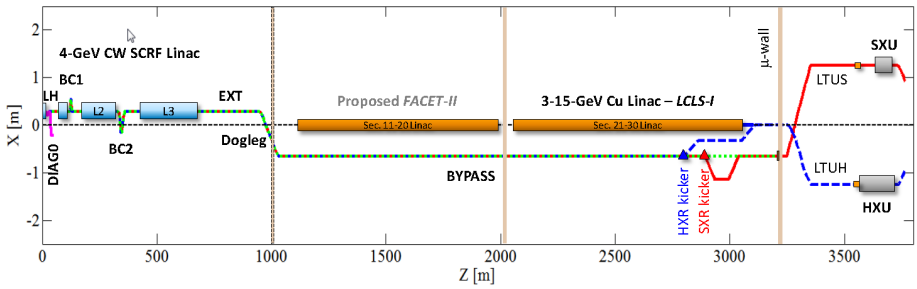

Figure 1: Top view of the LCLS-II (blue/red/green lines) with the existing LCLS linac and future FACET-II at SLAC.

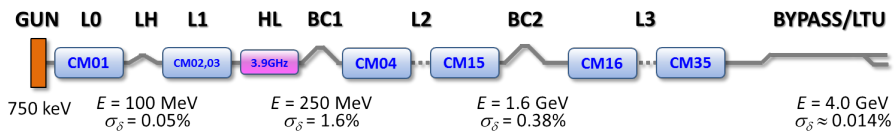

Figure 2: Schematic of the LCLS-II SCRF linac and bunch compressor system.

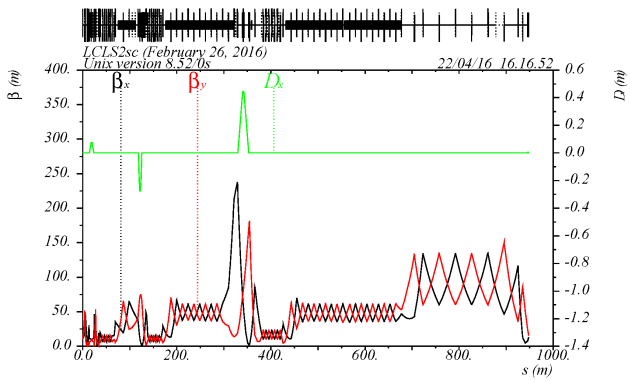

Figure 3: LCLS-II optics functions from injector to end of linac extension section.

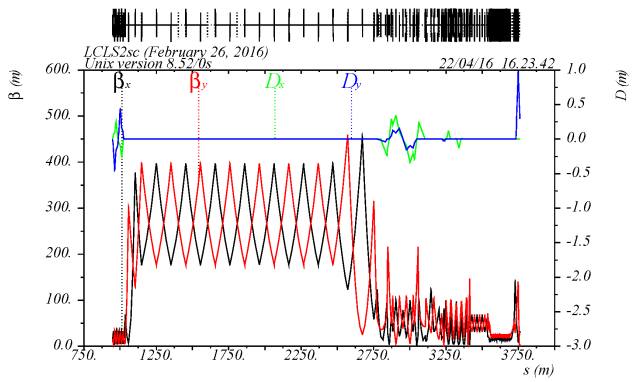

Figure 4: LCLS-II optics functions from bypass dogleg to HXR main dump.

TRANSPORT TO UNDULATORS

Downstream of the SCRF linac, the LCLS-II includes a dogleg which deflects the beam into the existing 2-km PEP-II electron bypass line, a 3-way beam spreader, HXR and SXR doglegs directing the beams to undulators, and the 120-kW main dump lines. An example of the HXR optics, from the dogleg to the main dump, is shown in Fig. 4.

The bypass dogleg is made of two rolled dipoles separated by a FODO quadrupole optics with a +I transfer matrix for cancelation of 1st order dispersion in both planes. The dogleg brings the beam up into the 2-km bypass line located 1.64 m up and 0.93 m to the right of the SCRF linac axis. A previously considered [5] bunch compressor BC3 just downstream of the dogleg has been removed. The use of the bypass avoids interference with the FACET-II Cu-linac in the same tunnel. The bypass consists of a 2-inch diameter pipe with a quadrupole, BPM, and steering coils every 101.6 m. The long 45° FODO cells yield a rather high (300 m) mean beta function. Four wire scanners and four adjustable-gap collimators are included in this line for emittance measurement at low beam power and for removal of beam halo. Positions of these devices have been adjusted to avoid interference with the FACET-II.

The bypass line brings the beam to a 3-way beam spreader at the end of the LCLS Cu-linac. Its function is to provide a high-rate, bunch-by-bunch deflection into separate lines leading either to the HXR or SXR undulator or to a 250-kW dump. Several modifications have been made to the spreader since its initial design [5]. First, a magnetic kicker has been adopted for fast beam deflection. It satisfies the specifications and is lower in cost compared to an RF deflector. Secondly, the HXR and SXR kickers, initially clustered together, have been separated by about 87 m in space. This reduces the maximum beam offset inside the 10-mm kicker aperture and avoids the impact of SXR kicker remnant fields on the HXR bunches. Two quadrupoles have been added between the two kicker systems to match the beta functions. The 4-GeV design includes three 1-m kicker magnets per HXR and SXR providing 0.75 mrad vertical kick. Additional space is reserved for future expansion to a 5-kicker system at a higher energy. Vertical beta functions at the kickers have been reduced by a factor of 7 since the initial design for more realistic tolerances on kicker stability (≃0.01%).

ISBN 978-3-95450-147-2

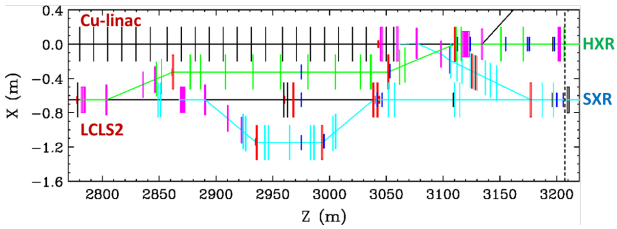

Figure 5: Top view of the LCLS-II spreader and the Cu-linac. The different lines are at different vertical positions.

Top view of the spreader is shown in Fig. 5. The kicker-deflected bunches are directed towards the HXR or SXR using Lambertson septum magnets, while the un-deflected bunches proceed to the new 250-kW dump that will be installed in the existing BSY muon wall. A BPM is included between the kicker and septum for measurement of deflected and un-deflected beam orbits. The LCLS-II baseline also includes the option of feeding the HXR undulator with a 120-Hz, 3-15 GeV beam from the existing LCLS Cu-linac when the SCRF HXR kicker and the last crossover DC bend are turned off. Future upgrade options may include the use of the CuRF beam in the SXR with the recently designed Cu-linac to SXR crossover dogleg; and a kicker system downstream of the HXR crossover for deflecting the SCRF or CuRF beam into the existing A-line (short black line at top of Fig. 5). The Cu-linac is $\simeq 65$ cm below the bypass; the SCRF-to-SXR line is at the bypass level; the SCRF-to-HXR crossover and the BSY dump line descend to the Cu-linac level; and the CuRF-to-SXR crossover climbs to the bypass level. All the spreader lines are designed to be first-order achromats and isochronous ($R_{56} = 0$) to mitigate microbunching effects.

The spreader connects to the downstream HXR and SXR LTU (H/S) lines leading to the undulators. The LTUH is the existing LCLS transport line. The LTUS will be a new line to the SXR; its optics has not been significantly changed since its initial design [5]. Each LTU consists of a horizontal dogleg providing 2.5-m horizontal separation between the HXR and SXR undulators, a 45° FODO section with four wire scanners for emittance diagnostics, and two weak vertical dipoles to remove a small incoming vertical slope and set the undulators into the same horizontal plane. One update in the LTU is a new arrangement of beam halo collimators which eliminates any collimator downstream of the last dipole before the undulators. This scheme will prevent secondary particles, generated by the collimators, from reaching the permanent-magnet undulators.

New HXR and SXR variable-gap, planar, permanent-magnet hybrid undulators will be installed side-by-side in the existing LCLS undulator hall as shown in Fig. 6. The SXR horizontal undulator will contain 21 undulator cells plus one empty cell for a self-seeding monochromator. Each 4.4-m cell includes a 3.4-m undulator with 39-mm period and 7.2-mm full magnetic gap, a quadrupole, a phase shifter, an RF BPM, a beam loss monitor, and X & Y steering coils. There are an additional 9 empty cells upstream and 3 cells downstream of the SXR undulator which may be used for a future undulator extension. An important recent update is made to the HXR, where a horizontal-gap vertically polarizing undulator (HGVPU) has been adopted. The advantage of the HGVPU is that it is more compact, better suited to the existing LCLS mechanical system, and expected to improve the photon efficiency. Position of the HGVPU has been optimized to fit on the present LCLS girders. The HGVPU will have 32 undulator cells plus 2 empty cells for self-seeding. There are four empty cells downstream of the HGVPU for a future extension. The HGVPU period (26 mm) and gap (7.2 mm) are the same as in the previous undulator design. Both undulators will be independently tunable by means of the electron beam energy and the adjustable undulator gap.

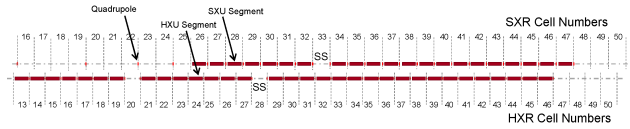

Figure 6: Schematic layout of the LCLS-II undulators [9].

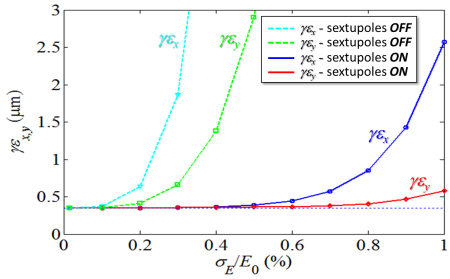

Figure 7: SXR normalized emittance versus rms energy spread with and without correction of 2nd order dispersion.

After the undulators the electron beams are deflected both horizontally and vertically towards the HXR and SXR dumps by means of rolled bends. A "soft" bend is included upstream of the main bends to prevent the coherent edge radiation from the main bends from reaching the downstream experimental areas. The dump line includes an OTR screen where the vertical dispersion is large for measurement of electron beam energy spread. The HXR line also provides a bunch length diagnostic using the existing X-band TCAV deflector and the OTR, where the optics has been optimized for the best resolution [10]. The XTCAV is also planned for the SXR.

Recent studies revealed that the LCLS-II dipoles downstream of the SCRF linac were the source of additional microbunching effects as well as large emittance growth under conditions with large energy chirp. Solution to the first problem has been found in the form of seven weak 4-bend chicanes placed next to the dipoles in the bypass and LTU doglegs [11]. The chicane strengths were optimized to nearly cancel the local R_{56} term created by the dipoles. The growth of emittance with energy spread was resolved by locally cancelling the 2nd order dispersion using additional sextupoles in the bypass dogleg, spreader and LTUS. The resulting momentum bandwidth is >0.5% as shown in Fig. 7.

REFERENCES

[1] T.O. Raubenheimer, "LCLS-II: status of the CW X-ray FEL upgrade to the SLAC LCLS facility," in *Proc. 37th Int. Free Electron Laser Conf. (FEL'15)*, Daejeon, Korea, Aug. 2015, paper WEP014, pp. 618–624.

[2] P. Emma *et al.*, "First lasing and operation of an angstrom-wavelength free-electron laser," *Nature Photonics*, vol. 4, pp. 641-647, Aug. 2010.

[3] "PEP-II Conceptual Design Report," SLAC, Stanford, CA, USA, Rep. SLAC-418, Jun. 1993.

[4] "Preliminary Conceptual Design Report for the FACET-II Project at SLAC National Accelerator Laboratory," SLAC, Stanford, CA, USA, Rep. SLAC-R-1067, Apr. 2016.

[5] Y. Nosochkov, P. Emma, T. Raubenheimer, and M. Woodley, "Design of the LCLS-II electron optics," in *Proc. 5th Int. Particle Accelerator Conf. (IPAC'14)*, Dresden, Germany, Jun. 2014, paper THPRO034, pp. 2940–2942.

[6] `http://tesla.desy.de/new_pages/TDR_CD/start.html`

[7] `http://www.linearcollider.org/`

[8] `http://www.xfel.eu/`

[9] H.-D. Nuhn and M. Rowen, private communication, 2015.

[10] Y. Ding, P. Emma, H. Loos, Y. Nosochkov, and J. Wang, "X-band RF transverse deflectors for the LCLS-II," SLAC, Stanford, CA, USA, SLAC note LCLSII-TN-15-42, Sep. 2015.

[11] J. Qiang *et al.*, "Design optimization of compensation chicanes in the LCLS-II transport lines," presented at the 7th Int. Particle Accelerator Conf. (IPAC'16), Busan, Korea, May 2016, paper TUPOR018, this conference.

ISBN 978-3-95450-147-2